

RESEARCH

Open Access



Hypertonicity induces mitochondrial extracellular vesicles (MEVs) that activate TNF- α and β -catenin signaling to promote adipocyte dedifferentiation

Guopan Liu^{1,2}, Ying Wang^{1,2}, Yilin Pan^{1,2}, Li Tian^{1,2}, Ming Ho Choi¹, Li Wang¹, Jin Young Kim¹, Jian Zhang³, Shuk Han Cheng¹ and Liang Zhang^{1,2*} 

Abstract

Background Recent studies demonstrated that elevated osmolarity could induce adipocyte dedifferentiation, representing an appealing procedure to generate multipotent stem cells. Here we aim to elucidate the molecular mechanisms that underlie osmotic induction of adipocyte reprogramming.

Methods To induce dedifferentiation, the 3T3-L1 or SVF adipocytes were cultured under the hypertonic pressure in 2% PEG 300 medium. Adipocyte dedifferentiation was monitored by aspect ratio measurement, Oil Red staining and qPCR to examine the morphology, lipid droplets, and specific genes of adipocytes, respectively. The osteogenic and chondrogenic re-differentiation capacities of dedifferentiated adipocytes were also examined. To investigate the mechanisms of the osmotic stress-induced dedifferentiation, extracellular vesicles (EVs) were collected from the reprogramming cells, followed by proteomic and functional analyses. In addition, qPCR, ELISA, and TNF- α neutralizing antibody (20 ng/ml) was applied to examine the activation and effects of the TNF- α signaling. Furthermore, we also analyzed the Wnt signaling by assessing the activation of β -catenin and applying BML-284, an agonist of β -catenin.

Results Hypertonic treatment induced dedifferentiation of both 3T3-L1 and the primary stromal vascular fraction (SVF) adipocytes, characterized by morphological and functional changes. Proteomic profiling revealed that hypertonicity induced extracellular vesicles (EVs) containing mitochondrial molecules including NDUFA9 and VDAC. Functionally, the mitochondrial EVs (MEVs) stimulated TNF- α signaling that activates Wnt- β -catenin signaling and adipocyte dedifferentiation. Neutralizing TNF- α inhibited hypertonic dedifferentiation of adipocytes. In addition, direct activation of Wnt- β -catenin signaling using BML-284 could efficiently induce adipocyte dedifferentiation while circumventing the apoptotic effect of the hypertonic treatment.

Conclusions Hypertonicity prompts the adipocytes to release MEVs, which in turn enhances the secretion of TNF- α as a pro-inflammatory cytokine during the stress response. Importantly, TNF- α is essential for the activation of the Wnt/ β -catenin signaling that drives adipocyte dedifferentiation. A caveat of the hypertonic treatment is apoptosis, which could be circumvented by direct activation of the Wnt/ β -catenin signaling using BML-284.

*Correspondence:

Liang Zhang
liangzhang.28@cityu.edu.hk

Full list of author information is available at the end of the article



© The Author(s) 2023. **Open Access** This article is licensed under a Creative Commons Attribution 4.0 International License, which permits use, sharing, adaptation, distribution and reproduction in any medium or format, as long as you give appropriate credit to the original author(s) and the source, provide a link to the Creative Commons licence, and indicate if changes were made. The images or other third party material in this article are included in the article's Creative Commons licence, unless indicated otherwise in a credit line to the material. If material is not included in the article's Creative Commons licence and your intended use is not permitted by statutory regulation or exceeds the permitted use, you will need to obtain permission directly from the copyright holder. To view a copy of this licence, visit <http://creativecommons.org/licenses/by/4.0/>. The Creative Commons Public Domain Dedication waiver (<http://creativecommons.org/publicdomain/zero/1.0/>) applies to the data made available in this article, unless otherwise stated in a credit line to the data.

Keywords Multipotent stem cells, Adipocyte dedifferentiation, Hypertonic treatment, Mitochondrial EVs, TNF- α , Wnt/ β -catenin signaling

Background

With a mesenchymal origin, adipocytes are recognized as an essential energy storage entity as well as a critical endocrine source that regulates systemic metabolism [1]. Despite the essential physiological functions, hypertrophy and hyperproliferation of adipose tissues lead to obesity, which is a major risk factor for a series of diseases including dyslipidemia, cardiovascular disease, type 2 diabetes and cancer [2–4]. At the cellular level, obesity is underlined by the deregulation of adipogenesis, the differentiation of committed pre-adipocytes into mature adipocytes [5, 6]. Interestingly, adipocytes do not remain at a static stage of terminal differentiation after adipogenesis. Instead, mature adipocytes display a high degree of plasticity and can be reverted to a multipotent progenitor-like state [1], which is termed adipocyte dedifferentiation and has been broadly observed *in vitro* and *in vivo* [7]. For example, during late pregnancy and lactation, mammary adipocytes lose lipid droplets and dedifferentiate into fibroblast-like preadipocytes that later re-differentiate into adipocytes after lactation [8]. Moreover, recent studies observed adipocyte dedifferentiation in the development of different malignant tumors, which was associated with the activation of Wnt signaling [9, 10] and Notch signaling [11]. A better understanding of adipocyte differentiation/de-differentiation balance holds the key to effectively preventing/treating obesity and related diseases.

The mechanisms of adipogenesis have been extensively investigated [12, 13]. However, much less is known about the molecular mechanisms underlying adipocyte dedifferentiation. Generally, pro- and anti-adipogenic genes/pathways play opposite roles in adipocyte dedifferentiation. For example, C/EBP β and PPAR γ are key pro-adipogenic genes and are typically suppressed to allow adipocyte dedifferentiation. As a PPAR γ agonist, rosiglitazone could block adipocyte dedifferentiation and tumor development in the Notch-driven liposarcoma mouse model [11]. In contrast, canonical Wnt/ β -catenin signaling ligands are recognized as anti-adipogenic factors and have been identified as enhancers of dedifferentiation. While overexpression of Wnt1 gene inhibited adipogenic differentiation of progenitor cells, exogenous application of Wnt3a could induce dedifferentiation of both mouse 3T3-L1 and human adipocytes [9, 14, 15]. In addition to Wnt signaling, Notch, TGF- β and TNF- α signaling have all been reported to suppress adipogenesis and promote adipocyte dedifferentiation in various

contexts [11, 15–17]. The detailed mechanism of how different signaling pathways cooperatively regulate adipocyte differentiation warrants further investigation.

Several methods have been established to induce adipocyte dedifferentiation, facilitating the investigation of molecular and cellular mechanisms. The “ceiling culture” of mature adipocytes was originally reported to induce the loss of lipid droplets and the emergence of progenitor-like cells, namely dedifferentiated fat cells (DFAT cells) [18]. Activation of TGF- β 1 signaling and different collagens were shown to regulate DFAT cells of the ceiling culture system [19]. Recently, physical changes in microenvironment, including matrix stiffening, increased compressive force, and elevated osmotic pressure, have been shown to affect the cell fate and adipocyte dedifferentiation [20, 21]. Accordingly, hypertonic treatment has been shown to induce osmotic stress and promote adipocyte dedifferentiation [22]. Given the ample cellular abundance and the simple operation, hypertonicity-induced DFAT holds a strong promise to transform regenerative medicine [23]. Mechanistically, activation of the anti-adipogenic Wnt/ β -catenin signaling was observed during the osmotic reprogramming of adipocytes. However, it remains elusive how hypertonicity activates the Wnt/ β -catenin signaling and drives the dedifferentiation.

In this study, we investigated the mechanism underlying hypertonicity-induced reprogramming of adipocytes. We first established a robust cellular model whereby high-osmolarity could efficiently induce dedifferentiation of 3T3-L1 and stromal vascular fraction (SVF)-derived adipocytes. We then conducted a proteomic profiling of extracellular vesicles (EVs) released from the dedifferentiating adipocytes receiving hypertonic treatment. Intriguingly, this showed that hypertonicity prompts the adipocytes to eject mitochondria via EVs, which in turn enhance the secretion of TNF- α cytokine during the stress response. Importantly, hypertonicity-induced EVs and TNF- α are critical for the activation of the Wnt/ β -catenin signaling that drives adipocyte dedifferentiation. Overall, our study defined a novel mitochondria-TNF- α axis that underlies the osmotic regulation of Wnt/ β -catenin signaling and adipocyte dedifferentiation.

Methods

Cell culture

3T3-L1 (ATCC CL-173) cells were cultured in DMEM medium (Thermo Fisher, product no. 11965126)

containing 10% FBS and 1% penicillin – streptomycin (all obtained from Thermo Fisher).

Stromal vascular fraction (SVF) isolation

All animal experiments were performed in accordance with the protocol approved by the Institutional Animal Research Ethics Sub-Committee of City University of Hong Kong and Department of Health of the Hong Kong Special Administrative Region. C57BL/6 J mice were used for this study and maintained in a 12:12 h light–dark cycle. 6 to 8-week-old females were anesthetized with 4% of isoflurane by inhalation, and then inguinal, retroperitoneal WAT were removed. The tissues were washed in sterile PBS, shredded and incubated in collagenase type II (Sigma, product no. C6885) for 1 h at 37 °C before passed through a sterile 100 µm filter. SVF was obtained after 5 min centrifugation at 1000 rpm. Culture medium (DMEM supplemented with 10% FBS and 1% penicillin – streptomycin (all obtained from Thermo Fisher) was added to resuspend the cells, followed by culturing in 100 mm culture dishes. The following day, the culture medium was changed to remove the dead and non-adherent cells.

3T3-L1 and SVF differentiation

1.25×10^5 of 3T3-L1 were seeded in 6-well dishes and cultured at 37 °C and 5% CO₂. To begin the differentiation, 10 µg/ml insulin (MedChemExpress, product no. HY-P0035), 1 µM dexamethasone (MedChemExpress, product no. HY-14648), 0.5 mM 3-isobutyl-1-methylxanthine (IBMX) (MedChemExpress, product no. HY-12318) and 2 µM rosiglitazone (Sigma, product no. R2408-10MG) (Differentiation medium) were supplemented to the culture medium to constitute the differentiation medium for 2 days. For differentiation of SVF, the SVF cells were incubated for 5 days with differentiation medium. The medium was then changed to DMEM containing 10% FBS, 1% penicillin – streptomycin, and 10 µg/ml insulin for 48 h followed by changing to the culture medium.

Oil Red O staining

Adipocytes were stained with Oil red O staining kit (Solarbio, product no. G1262) solution to detect the lipid droplets according to manufacturer's instructions. Specifically, cells were fixed with 10% formalin for 20 min at room temperature, followed by washing with 60% isopropanol for 5 min. Subsequently, staining was conducted with ORO solution for 20 min at room temperature to enable binding of the dye to the lipid droplets. Finally, the

cells were washed with distilled water to eliminate any residual dye.

Hypertonic-induce dedifferentiation of adipocytes

To induce hypertonic shock, adipocytes were treated with a medium containing 2% polyethylene glycol 300 (PEG 300) diluted in culture medium. Specifically, adipocytes were exposed to the hypertonic dedifferentiation medium, composed of DMEM supplemented with 10% FBS and 1% penicillin–streptomycin (all obtained from Thermo Fisher) and 2% PEG-300 (MedChemExpress, product no. HY-Y0873), and maintained at 37 °C and 5% CO₂. The medium was changed every 3 days, being careful to avoid shaking the dish to allow the hypertonic medium to diffuse slowly in the culture dish.

Osteogenic differentiation

To induce osteogenic differentiation, 1×10^6 cells were seeded in 6-well plates and incubated overnight at 37 °C and 5% CO₂. The culture medium was then replaced with StemPro Osteogenesis Differentiation medium (Thermo Fisher, product no. A1007201) and cells were maintained in this medium for up to 14 days, with medium renewal every 3 days. This medium contains specific factors that promote differentiation toward the osteogenic lineage, allowing the cells to deposit mineralized extracellular matrix and express osteogenic markers.

Alkaline phosphatase assay

Alkaline phosphatase (ALP) staining was conducted on Day 9 of the feeder cell-mediated reprogramming process, following the manufacturer's instructions for the Alkaline Phosphatase Detection Kit (Sigma, product no. SCR004). The staining was performed to detect the activity of ALP, a marker of pluripotency, and to assess the success of the reprogramming process.

MitoTracker staining

To stain cells with MitoTracker (CST, product no. FM 9074), the 1 mM stock solution should be diluted directly into normal growth media to achieve a staining concentration ranging from 400 nM. The live cells were incubated for 15 min at 37 °C. Following incubation, live imaging is necessary to visualize the staining pattern within the cells.

qPCR gene expression analysis

Total RNA was isolated using the RNA Extraction Kit (Takara, product no. 9767) in accordance with the manufacturer's recommended protocol. The first-strand

cDNA was synthesized using the PrimeScript RT Reagent Kit (Takara, product no. RR047A) for RT-PCR. In brief, a 10 μ L system containing 2 μ L of 5 \times PrimeScript RT Master Mix (Perfect Real Time) and RNase-Free Distilled Water and RNA solution, with a total RNA amount of 500 ng, was transferred to the ABI ProFlex PCR System (2 \times 96-well) for reverse transcription. RT-PCR was then conducted using the Ex-Taq PCR kit (Takara, product no. RR820A) following the manufacturer's instructions. All RT-qPCR primer sequences were included in Additional file 2: Table S1.

Western blotting

To obtain lysates, cells were washed twice with cold PBS and lysed with 1 mL of RIPA buffer (Beyotime, product no. P0013B) at 4 °C for 1 h with gentle rotation. The lysate was subsequently centrifuged at 12,000g for 20 min at 4 °C, and the resulting supernatant was quantified the protein concentration. Protein extracts were then separated by SDS-PAGE and transferred onto a NC membrane (Bio-Rad, product no. 1620112). The membranes were incubated overnight at 4 °C with antibodies against VDAC (CST, product no. 4866 s, 1:1000), NDUFA9 (Abcam, product no. ab14713, 1:1000), CD81 (Santa Cruz, product no. sc-166029, 1:1000), Non-phospho (Active) β -Catenin (CST, product no. 8814, 1:2000), β -Catenin (CST, product no. 9562, 1:1000) and β -actin (Santa Cruz, product no. sc-47778, 1:1000). Following incubation with the appropriate secondary antibody (Abcam, product no. ab205719; Thermo Fisher, product no. 31460, 1:4000), the protein bands were visualized using an enhanced chemiluminescence (ECL) kit (Bio-Rad, product no. 170-5061) and captured using a Bio-red ChemiDoc.

Chemical treatments

To inhibit EV secretion, adipocytes were treated with 10 μ M GW4869 (Sigma-Aldrich, product no. D1692) in isotonic and hypertonic cultures. For control treatments, an equivalent volume of DMSO was added. After two days, the media were collected for EVs isolation and analysis.

To mitigate mitochondrial stress, adipocytes were treated with 1 mM pyruvic acid (Sigma-Aldrich, product no. 107360) in hypertonic cultures. For control treatment, an equivalent volume of DMSO was added. The treated cells were subjected to MTG staining, and the media were collected for EVs isolation and analysis.

EVs isolation and protein digestion

The 3T3-L1 adipocytes were treated by isotonic and hypertonic medium. After 48 h culture, conditional mediums were collected. The EVs were isolated by a sequential ultracentrifugation includes removing

supernatant by 300 g for 10 min, 2000 g for 15 min, 10000 g for 70 min and collecting the sediment by 120000 g for 2 h. The pellets were washed once with PBS and precipitated at 120000 g for 70 min. Purified EVs pellets were vacuum dried and then were resuspended in 100 μ L of buffer containing 8 M urea (Sigma, product no. U1250) and 50 mM NH_4HCO_3 (Alfa Aesar, product no. 14249). The resuspended suspensions contain \sim 80 μ g protein each as determined by DC protein assay (Bio-Rad, product no. 5000114). In-solution digestion was performed for the following LC-MS/MS analysis. Briefly, the EVs protein suspensions were reduced with 20 mM DTT for 10 min at 95 °C, followed by alkylation with 50 mM IAA for 30 min at RT in dark. The solutions were then diluted with 50 mM NH_4HCO_3 buffer (pH 8.0) to make the urea concentration lower than 1 M. MS-grade trypsin (Thermo Fisher, product no. 90058) coupled with Lyc-C protease was added into the solution (pH 8.0) at an enzyme/protein ratio of 1:25 to digest the protein at 37 °C overnight. The resulting peptide samples were desalted using C18 tips (Thermo Fisher, product no. 87784) and resuspended with 0.1% formic acid buffer (Thermo Fisher, product no. 85178) for LC-MS/MS analysis.

LC-MS/MS analysis

The peptide samples were analyzed using EASY-nLC 1200 system combined with a Q Exactive HF mass spectrometry (Thermo Scientific). For each injection, 6 μ L loading sample containing around 0.5 μ g peptide was separated by a C18 nano-column (250 nm, 75 μ m, 3 μ m, PepSep, Denmark) (Thermo Fisher, product no. 87784) at a flow rate of 250 nl/min. The 75 min reversed-phase gradient was achieved by mobile phase A (0.1% formic acid in ultrapure water) and mobile phase B (0.1% formic acid/80% acetonitrile in ultrapure water). MS recording was operated in the range of 350 to 1800 m/z with a mass resolution of 120,000. The positive ion mode was employed with the spray voltage at 2000 V and a spray temperature of 320 °C. The resolution of dd-MS2 was 30,000 with a 1×10^5 of AGC target. The Maximum IT was set at 60 ms, and the loop count was 12. The isolation window was 1.6 m/z, and the fixed first mass was 120.0 m/z.

Database search

Raw files created by XCalibur 4.0.27 (Thermo Fisher) software were analyzed using Proteome Discoverer software (version 2.2, Thermo Fisher) against the UniProt mouse protein database in Sequest HT node. The precursor and fragment mass tolerances were set to 10 ppm and 0.02 Da, respectively. A maximum of two missed cleavage sites of trypsin was allowed. Carbamidomethylation (C) was set as static modification, and oxidation (M) and

acetyl (protein N terminal) were set as variable modifications. The false-discovery rates (FDRs) of peptide spectrum matches (PSMs) and peptide identification were determined using the Percolator algorithm at 1% based on *q* value. For label-free quantification, the Minora Feature Detector node was used in the processing workflow, and the Precursor Ions Quantifier node and the Feature Mapper node in the consensus workflow. Normalization of the quantitative values was performed in Proteome Discoverer, based on the total peptide intensity of the samples.

Transmission electron microscopy analysis of extracellular vesicle

EVs were fixed with a solution of 5% formaldehyde and 2% glutaraldehyde in 0.1 M cacodylate buffer (pH 7.2) overnight at 4 °C. After washing with 0.1 M cacodylate buffer, the samples were further fixed with a solution of 2% osmium tetroxide in 0.1 M cacodylate buffer for 2 h at room temperature, in the dark. Following another wash with 0.1 M cacodylate buffer, the samples were dehydrated using a series of ethanol solutions with increasing concentrations (30%, 50%, 70%, 80%, 90%, 95%, and 100%) and further dehydrated with 70% and 100% acetone. The samples were then infiltrated with Spurr's resin at increasing concentrations of 25%, 50%, 75%, and 100%. After polymerization for 2 days at 70 °C, ultrathin sections were prepared using a diamond knife, collected onto butvar-coated 100 mesh grids (EMS, product no. FF100-CU), and counterstained with UranylLess (EMS, product no. 22409) for 10 min and lead citrate for 1 min. Finally, the samples were imaged using a transmission electron microscope (Philips Technai 12) to visualize the internal structure and morphology of the EVs.

Results

Hypertonicity induced dedifferentiation of 3T3-L1 adipocytes

Previous studies have reported that the physical compression induced by hypertonic treatment could lead to dedifferentiation of adipocytes derived from primary sources

[21]. However, this phenomenon has not been recapitulated in cell line models. To address this, we examined whether hypertonic treatment could induce dedifferentiation of the well-established 3T3-L1 adipocytes model. We included adipocytes derived from the stromal vascular fraction (SVF) as the positive control. The experimental flow is illustrated in Fig. 1A. Briefly, 3T3-L1 and SVF cells were subject to adipogenic differentiation for 7 days, resulting in adipocytes with visible accumulation of lipid droplets and round morphology. We then started the dedifferentiation process of the adipocytes using hypertonic treatment with 2% PEG-300 in culturing media as describe before [21, 24]. Over four to seven days of hypertonic treatment, about 40–70% of the 3T3-L1 and SVF adipocytes lost lipid droplet, which were significantly higher than the control isotonic treatments (Fig. 1B, C). At the end of the 7-day treatment, we conducted Oil Red O staining which confirmed the depletion of lipid contents (Fig. 1D) and adipocytes (Fig. 1E). In parallel, we observed a significant increase in the aspect ratios of cells in the hypertonic treatment group (Fig. 1F), which is in line with the elongated morphologies of dedifferentiated adipocytes reported in previous studies [9, 25]. To validate the dedifferentiation of the 3T3-L1 adipocytes, we examined the expression of adipocyte marker genes. Compared with the isotonic control, hypertonic treatment of 3T3-L1 adipocytes led to 40–60% reductions in the expression of adipogenic markers, including *C/EBPβ*, *PPAR-γ*, and adiponectin (Fig. 1G). In parallel, we applied immunostaining to examine CD13 and Endoglin, which are surface markers of dedifferentiated adipocytes. Quantitative analysis revealed significantly higher expression of CD13 and Endoglin in adipocytes of the hypertonic treatment than the isotonic control (Additional file 2: Fig. S1A–D). Overall, these results indicated that hypertonic treatment could effectively induce dedifferentiation of 3T3-L1 adipocytes.

An important functional feature of the dedifferentiated adipocytes is the ability to re-differentiate into other mesenchymal lineages. Next, we evaluated the 3T3-L1 adipocytes for their capacity in osteogenic and

(See figure on next page.)

Fig. 1 Hypertonic treatment induces dedifferentiation of adipocytes. **A** A diagram depicts the experimental workflow. Following the adipogenic culture of 3T3-L1 and SVF cells, the adipocytes were treated with the hypertonic medium for another seven days, and the dedifferentiated cells are isolated for osteogenic differentiation. **B** Representative images of adipocytes in the hypertonic culture for the indicated time. Scale bar: 100 μm. **C** Quantification of adipocytes losing clear lipid droplets over time in the indicated culture conditions. Error bars represent SD (*n* = 3 independent experiments). **D** and **E** Images (D) and quantification (E) of Oil Red O staining of adipocytes following indicated treatments for seven days. **F** Box plots depict the aspect ratio of indicated adipocytes (*n* = 200 cells) following control or hypertonic treatments of four days. **G** RT-qPCR analysis of the expression of *C/EBPβ*, *PPARγ*, and adiponectin in isotonic and hypertonic treated adipocytes. **H** Representative images of alkaline phosphatase (ALP) staining showing the osteogenic potential of the de-differentiated 3T3-L1 adipocytes. **I** RT-qPCR analysis of the expression of Runx2 and ALP following osteogenic induction of isotonic and hypertonic treatment of 3T3-L1 adipocytes. **J** RT-qPCR analysis of the expression of Smad3, Col2a1 and Sox9 following chondrogenic induction of isotonic and hypertonic treatment of 3T3-L1 adipocytes

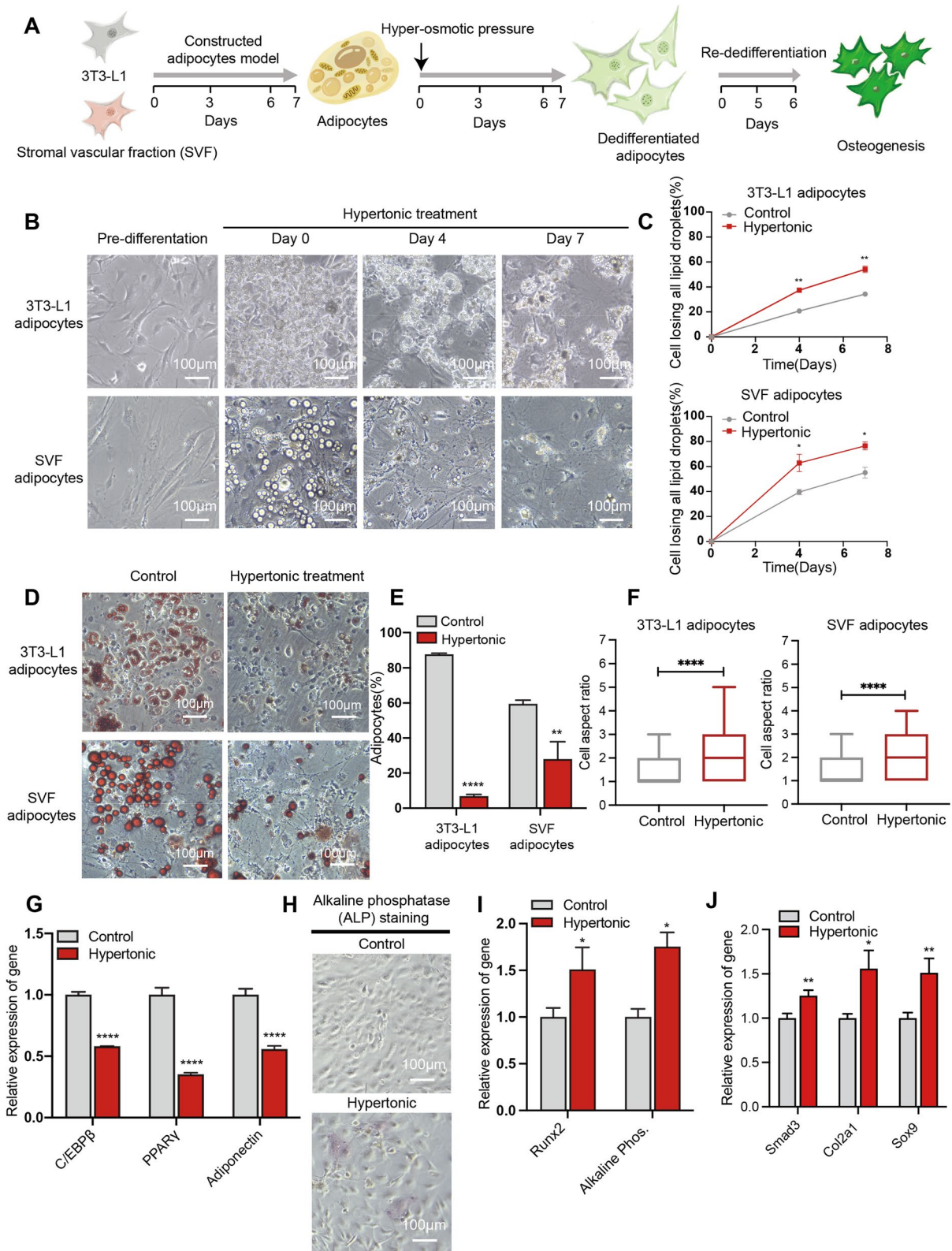


Fig. 1 (See legend on previous page.)

chondrogenic re-differentiation after hypertonic treatment. Osteogenic induction promoted the expression of alkaline phosphatase (ALP), a marker of the osteogenic lineage, in 3T3-L1 adipocytes receiving hypertonic treatment (Fig. 1H–I). This was accompanied by significantly increased expressions of Runx2, which is another osteogenic marker (Fig. 1I). In addition, chondrogenic induction of the 3T3-L1 adipocytes after hypertonic treatment led to an increased expression of chondrogenic marker genes, including Smad3, Col2a1 and Sox9 (Fig. 1J). Importantly, the control cells that received isotonic treatment did not display osteogenic nor chondrogenic differentiation capacity, in line with the adipogenic commitment of the 3T3-L1 cells. Taken together, we conclude that hypertonic treatment could effectively induce the multipotent dedifferentiation of 3T3-L1 adipocytes.

Adipocytes receiving hypertonic treatment eject mitochondria in extracellular vesicles

Cellular transformation is commonly accompanied by autocrine signaling activities [26]. Among them, extracellular vesicles (EVs) are a prominent mediator of cell–cell communication in many biological contexts including cancer [27]. To investigate whether EV factors may regulate the hypertonic dedifferentiation of adipocytes, we isolated the EVs from the isotonic or hypertonic treatments of 3T3-L1 adipocytes and compared their proteomic contents using LC–MS analysis (Fig. 2A). Overall, we identified 359 and 486 proteins (identified with ≥ 2 unique peptides) in the EVs from hypertonic- and isotonic-treated 3T3-L1 adipocytes, respectively. While 334 proteins were shared between the two EVs population, we observed 25 proteins that are uniquely present in the hypertonic EVs (Fig. 2B). Intriguingly, Gene Ontology (GO) term annotation of the 25 hypertonic-unique proteins revealed enrichment of mitochondrial components (Fig. 2B; Additional file 2: Table S2), which host the enzymatic complexes of oxidative phosphorylation and play a key role in ATP production and energy homeostasis of cells. In addition, quantitative analysis identified 47 proteins with $>$ tenfold upregulation in hypertonic EVs (Fig. 2C; Additional file 2: Table S3). Notably, GO term

analysis ascribed more than 50% of the hypertonically up-regulated EV proteins as components of the mitochondrion (Fig. 2D), including NDUFA9 and UQCRC2, which are components of the NADH-ubiquinone oxidoreductase (complex I) and the ubiquinol-cytochrome c reductase (complex III) on the mitochondrial inner membrane, respectively. These results suggest that adipocytes may eject mitochondrial components through EVs in response to hypertonic treatment.

Hypertonicity is known to disrupt the ionic homeostasis of cells and reduce the electronic potential in mitochondria, consequentially inhibiting ATP production [28]. Therefore, we examined the status of mitochondria in adipocytes using MitoTracker Green (MTG), a fluorescent probe that accumulates in live-cell mitochondria in an electronic-potential-dependent manner [29]. Compared to the isotonic control, hypertonic treatment markedly blocked MTG staining of mitochondria in adipocytes (Fig. 2E, F). Pyruvic acid is known to alleviate mitochondrial stress by improving electronic potential [30, 31], and application of pyruvic acid (1 mM) to the hypertonic treatment effectively restored MTG staining (Fig. 2E, F). These results suggested that hypertonicity treatment could lead to disrupted electronic potential and mitochondrial stress in adipocytes.

Recent investigations have revealed that a spectrum of cells could eject damaged mitochondria from their cytosol [32, 33]. Therefore, we hypothesized that adipocytes eject mitochondria in EVs in response to the hypertonic stress of mitochondria. To address this, we exploited electronic microscopy (EM) to examine the EVs released from 3T3-L1 adipocytes under hypertonic treatment and observed folded membranous structures that resemble mitochondrial cristae enclosed in EVs (Fig. 2G). In parallel, hypertonic treatment also increased the levels of mitochondrial proteins VDAC and NDUFA9 in the EVs of 3T3-L1 adipocytes, which were reduced by pyruvic acid that alleviates mitochondrial stress (Fig. 2H). At the same time, we did not observe differences in the levels of the pan-EV marker CD81, indicating the specific effects on the mitochondrial components. In addition, GW4869, a compound that blocks EVs secretion,

(See figure on next page.)

Fig. 2 Hypertonic treatment prompts adipocytes to eject mitochondria via EVs. **A** EVs from isotonic control and hypertonic culture of 3T3L1 adipocytes were subject to quantitative proteomic analysis. **B** Venn diagram compares the proteins of control and hypertonic EVs from adipocytes. The right graph depicts the GO-term analysis of the 25 hypertonic-unique proteins. **C** Scatter plot summarizes the differential analysis of the EVs proteome between the control and hypertonic pressure. Sloping dotted lines demarcate tenfold difference in the abundance. **D** GO-term analysis of the up-regulated proteins in the hypertonic EVs. The top five cellular components are shown. **E** and **F** The 3T3-L1 adipocytes receiving indicated treatments for 8 h were stained using MitoTracker Green (green) and DAPI (blue). Relative intensities of the green channel were quantified. Scale bars, 10 μ m. **G** Representative transmission electron microscopy (TEM) images of hypertonic EVs from 3T3-L1 adipocytes. Arrows indicate inclusions of mitochondria fragments. **H** Cell lysates and EVs of 3T3-L1 adipocytes following indicated treatments were subject to immunoblot analyses of the indicated proteins, respectively. Full-length blots are presented in Additional file 1: Additional file 1

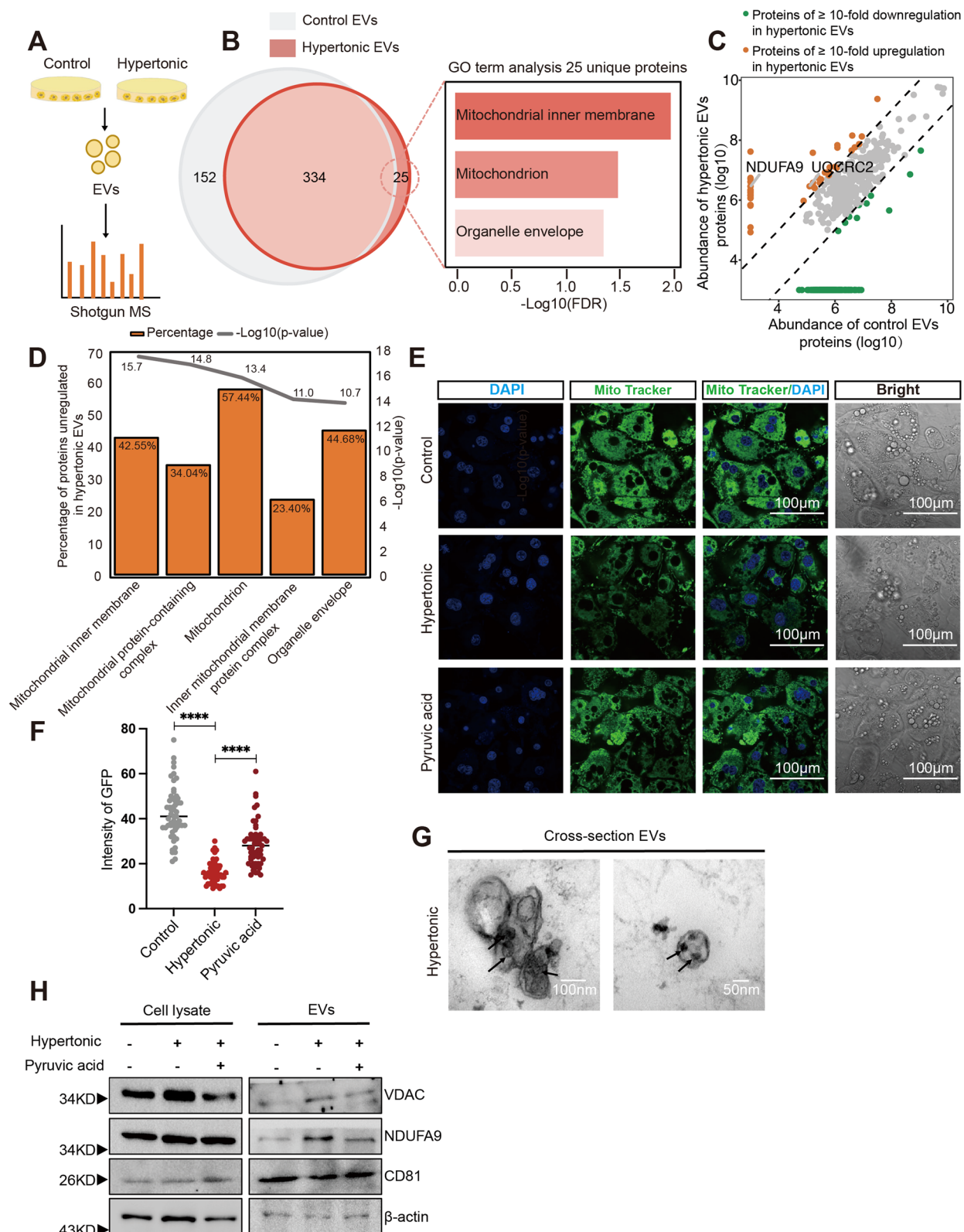


Fig. 2 (See legend on previous page.)

substantially inhibited the EVs level of NDUFA9 induced by hypertonic treatments (Additional file 2: Fig. S2). This supports that mitochondrial components were released through the EVs route during hyperosmotic stress. Taken together, these results suggest that hypertonic treatment leads to mitochondrial stress in adipocytes, resulting in ejection of mitochondrial components in EVs. We term these vesicles mitochondrial EVs (MEVs).

MEVs activate TNF- α signaling in promoting the hypertonicity-induced adipocytes dedifferentiation

EV-mediated transfer of mitochondrial contents has been shown to stimulate metabolic and inflammatory responses of recipient cells [34]. Therefore, MEVs could constitute an autocrine factor that regulates adipocyte dedifferentiation. To test this, we isolated MEVs from the hypertonic treatment of 3T3-L1 adipocytes and applied them to naïve 3T3-L1 adipocytes cultured in isotonic condition (Fig. 3A). After 72 h, RT-qPCR analysis revealed a significant reduction of the expression of adipogenic markers, including C/EBP β , PPAR- γ , and adiponectin (Fig. 3B). These results suggested a potential role of MEVs as the mediator of hypertonic-induced adipocyte dedifferentiation.

Extracellular mitochondria have been shown to promote inflammatory processes [35–37]. We next examined whether the hypertonic MEVs could influence the inflammatory pathways in adipocytes. Indeed, application of hypertonic MEVs to 3T3-L1 adipocytes significantly induced the expression of a series of inflammatory genes, including TNF- α , IL-6, RIP1, CEBPA, and MCP-1 (Fig. 3C; Additional file 2: Fig. S3A). In particular, a robust 4- and eightfold induction was observed for the key inflammatory genes TNF- α and IL-6 after 2-h MEVs treatment, respectively. The induction of both genes remained high at 8 h post treatment, suggesting the long-lasting effect of hypertonic MEVs. Importantly, reducing mitochondria stress by pyruvic acid prevented the hypertonic EVs from inducing TNF- α expression (Fig. 3D). Given that pyruvic acid decreases the mitochondrial contents in EVs, these results suggested that

hypertonic MEVs could stimulate inflammatory signaling in adipocytes.

Next, we examined the inflammatory responses of adipocytes in the hypertonic culture. Similar to the hypertonic EVs treatment, 2 h of hypertonic culture induced the expression of inflammatory genes TNF- α , IL-6, RIP1, CEBPA, and MCP-1 in 3T3-L1 adipocytes (Fig. 3E; Additional file 2: Fig. S3B). Interestingly, the expression levels of TNF- α , IL-6, CEBPA, and MCP-1 declined substantially after 8 h of hypertonic culture. This contrasted with the long-lasting effect of hypertonic EVs and could be due to adaptation of adipocytes to the relatively mild hypertonicity. Notably, addition of pyruvic acid to the hypertonic culture abolished the induction of TNF- α and IL-6 expression (Fig. 3F), further supporting the role of mitochondrial stress in the effects of hypertonicity. Importantly, ELISA assay revealed an increased level of TNF- α protein in the media of hypertonic-treated adipocytes (Fig. 3G). Altogether, these results indicated that hypertonic stress and mitochondrial EVs could activate inflammatory signaling in adipocytes.

TNF- α activates β -catenin to promote the hypertonicity-induced dedifferentiation of adipocytes

Previous studies have highlighted the anti-adipogenic activity of the TNF- α inflammatory signaling [17, 38]. To examine whether the role of TNF- α in hypertonicity-induced adipocyte dedifferentiation, we applied TNF- α neutralizing antibody to 3T3-L1 adipocytes in the hypertonic culture. Compared to the control antibody, TNF- α neutralizing antibody significantly inhibited the hypertonicity-induced expression of stem cell genes, including *Esrrb*, and *Sox2* (Fig. 4A). Though not significant, a modest reduction of *Smad9* was also observed after neutralizing TNF- α in the dedifferentiating adipocytes (Fig. 4A). These results pointed to a key role of TNF- α in hypertonicity-induced adipocyte dedifferentiation.

The Wnt/ β -catenin pathway is also known to inhibit adipogenesis [39] and promote the dedifferentiation of mature adipocytes [9]. In fact, activation of β -catenin was reported to underlie hypertonic dedifferentiation of adipocytes [21]. We then assessed the hypertonic EVs treatment for the influence on β -catenin in adipocytes.

(See figure on next page.)

Fig. 3 Hypertonicity and mitochondrial EVs (MEVs) activates TNF- α signaling in 3T3-L1 adipocytes. **A** EVs from control or hypertonic cultures of 3T3-L1 adipocytes were used to treat naïve 3T3-L1 adipocytes in isotonic culture. **B** RT-qPCR analysis of the expression of C/EBP β , PPAR γ , and adiponectin in 3T3-L1 adipocytes treated with EVs isolated from the indicated cultures. **C** RT-qPCR analysis of the expression of TNF- α and IL-6 in 3T3-L1 adipocytes treated with EVs isolated from the adipocytes from the indicated cultures. **D** RT-qPCR analysis of the expression of TNF- α in 3T3-L1 adipocytes receiving EVs from the indicated treatments. **E** RT-qPCR analysis of the expression of TNF- α and IL-6 in 3T3-L1 adipocytes receiving indicated treatments. **F** qPCR analysis of TNF- α related inflammatory factor in 3T3-L1 adipocytes receiving indicated treatments for 2 h. **G** ELISA analysis of the protein levels of TNF- α in the media of 3T3-L1 adipocytes receiving indicated treatments for 8 h

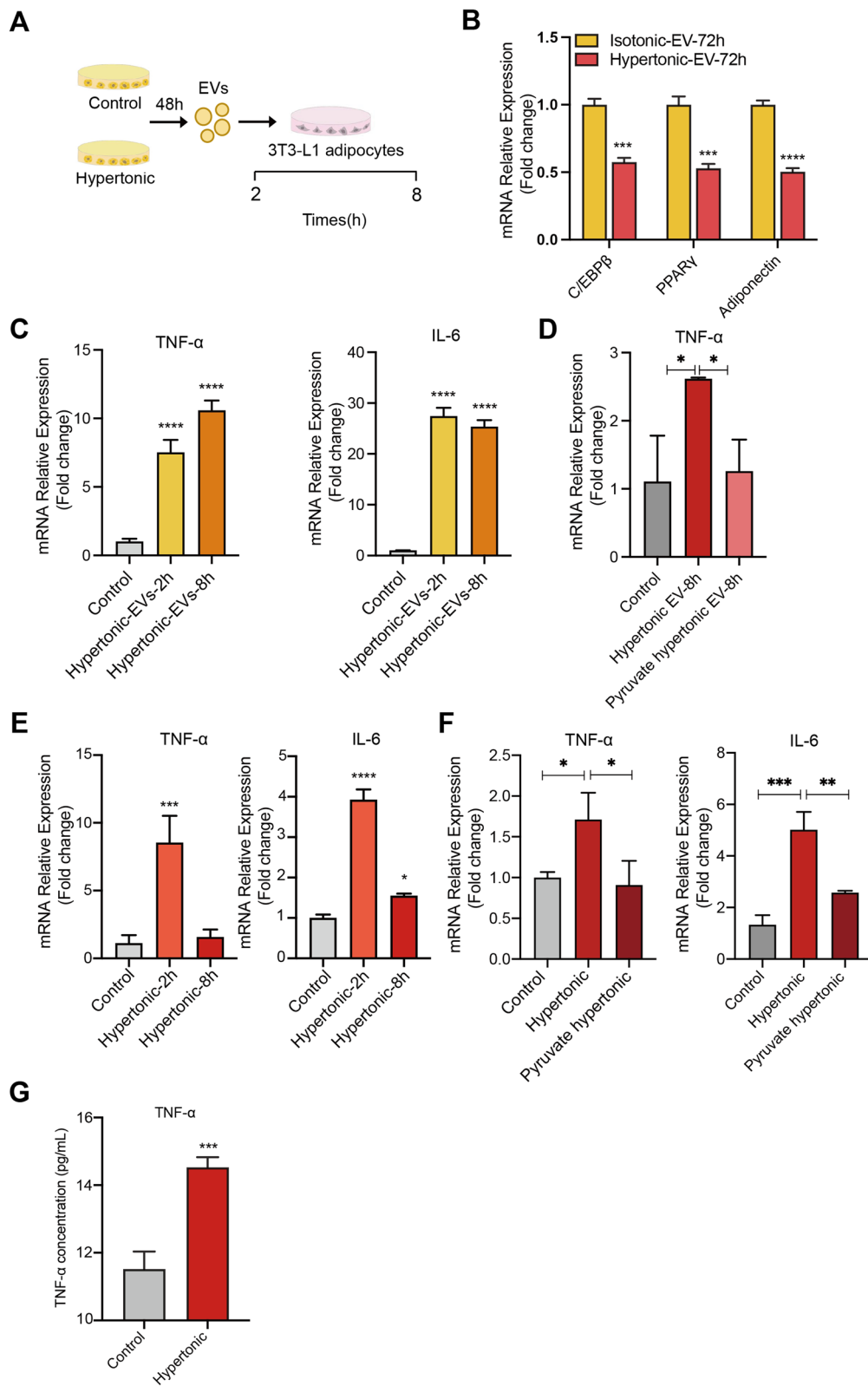


Fig. 3 (See legend on previous page.)

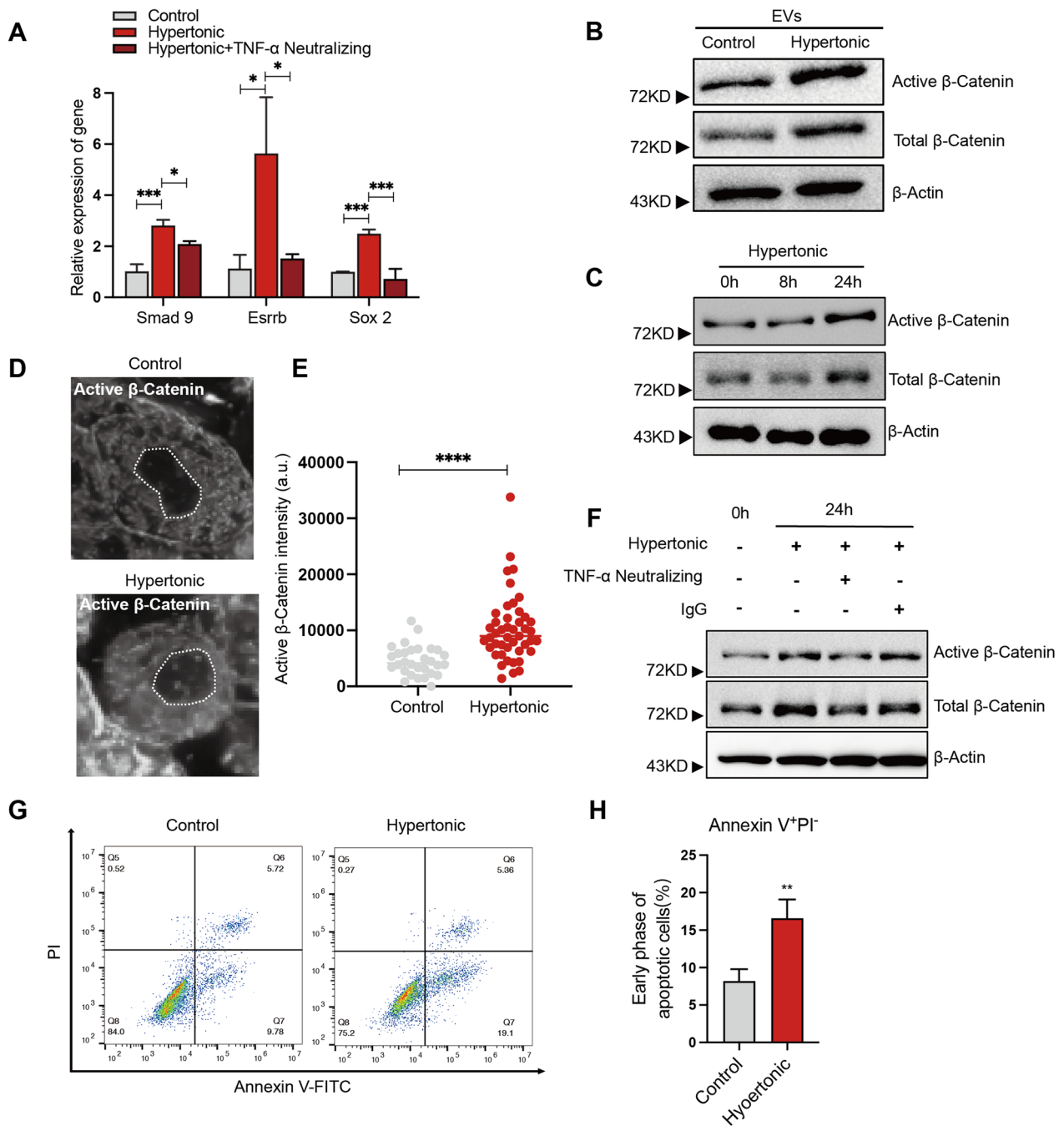


Fig. 4 TNF-α activates β-catenin and apoptosis in adipocytes under hypertonic treatment. **A** RT-qPCR analysis of the expression of Smad9, Esrrb and Sox2 in adipocytes receiving the indicated treatments. **B** Total cell lysates from 3T3-L1 adipocytes treated by EVs from isotonic or hypertonic adipocyte cultures were subject to western blot analyses of indicated proteins. Full-length blots are presented in Additional file 1: Additional file 2. **C** Total cell lysates from 3T3-L1 adipocytes in indicated culture conditions were subject to western blot analyses of indicated proteins. Full-length blots are presented in Additional file 1: Additional file 3. **D** Representative images of immunostaining of active β-catenin in 3T3-L1 adipocytes following control or hypertonic treatment. **E** Quantification of the intensity of active β-catenin staining in the nucleus of adipocytes following control or hypertonic treatment for 24 h. **F** 3T3-L1 adipocytes were treated with the indicated conditions for 24 h and the cell lysates were subject to western blot analysis of indicated proteins. Full-length blots are presented in Additional file 1: Additional file 4. **G** Representative results of annexin V/PI flow cytometry analysis of adipocytes receiving indicated treatments. **H** Bar graphs depict the proportions of cells in early-phase apoptosis in adipocytes receiving indicated treatment

Western blot demonstrated stabilization of β -catenin and accumulation of non-phosphorylated (active) β -catenin in 3T3-L1 adipocytes after 24 h of hypertonic MEVs treatment (Fig. 4B). This was also observed in 3T3-L1 adipocytes after 24 h of hypertonic culture (Fig. 4C). In parallel, immunostaining revealed that the nuclear accumulation of active β -catenin in hypertonic culture (Fig. 4D, E). Therefore, in addition to inducing TNF- α , hypertonic stress and the mitochondrial EVs also activate the anti-adipogenic Wnt/ β -catenin signaling.

TNF- α has been reported to induce the stabilization of β -catenin and inhibit adipogenesis [17]. Therefore, we assessed the importance of TNF- α in hypertonic activation of β -catenin during dedifferentiation of adipocytes. Indeed, application of the TNF- α neutralizing antibody markedly block the stabilization of total β -catenin and non-phosphorylated (active) β -catenin in hypertonic culture (Fig. 4F). These results demonstrate that TNF- α is essential for the hypertonic activation of Wnt/ β -catenin signaling that drives adipocyte dedifferentiation.

Hypertonic treatment induces apoptosis of adipocytes that is circumvented by direct activation of β -catenin signaling

The hypertonic dedifferentiation of adipocytes typically requires up to 7 days of culture in 2% PEG-300. Given that TNF- α is also known as a proinflammatory cytokine to induce apoptosis of adipocytes [40], we decided to examine the apoptotic status of adipocytes using the AnnexinV-FITC/PI staining. Compared to the isotonic control, we observed a significantly increase of cells in the early phase of apoptosis indicated by the AnnexinV staining (Fig. 4G, H). At the same time, we did not observe a difference in PI-positive cells in the early phase of apoptosis, which could potentially be due to the loss of such cells in the washing process prior to the harvest. We concluded that the extended hypertonic treatment could lead to apoptosis in parallel to dedifferentiation of adipocytes.

To circumvent the apoptotic effects of hypertonicity and TNF- α in inducing adipocyte dedifferentiation, we exploited BML-284, a small compound that stabilizes β -catenin and directly activates the Wnt/ β -catenin signaling. We treated 3T3-L1 and SVF adipocytes in isotonic cultures with BML-284 (10 mM) and examined the lipid droplets and morphological changes. Strikingly, 4 days of BML-284 treatment led to a significant disappearance of visible lipid droplets (Fig. 5A, B). This is accompanied by significant increases of cells with elongated morphology in BML-284-treated 3T3-L1 and SVF adipocytes (Fig. 5C). These results indicated the anti-adipogenic activity of BML-284, which was further supported by decreased Oil red staining (Fig. 5D, E). In parallel, we observed significant decreases in the expression of adipogenic genes (C/EBP β , PPAR- γ , and adiponectin) in conjunction to significant increases in the expression of marker genes (Smad9, Esrrb and Sox2) and proteins (CD13 and endoglin) of multipotency in BML-284 treated cells (Fig. 5F–G; Additional file 2: Fig. S4). Importantly, the re-differentiation assays revealed increased expression of osteogenic and chondrogenic markers in BML-284-treated adipocytes after inducing treatments correspondingly (Fig. 5H–J). Altogether, these results indicated that direct activation of β -catenin signaling by BML-284 could induce adipocyte dedifferentiation.

Next, we compared BML-284 and the hypertonic treatment for their effects on cell apoptosis. Notably, while the hypertonic treatment induced a significantly level of apoptosis in 3T3-L1 adipocytes, BML-284 did not lead to significant apoptosis (Fig. 5K, L). Overall, these results demonstrated that BML-284 treatment could effectively induce adipocyte dedifferentiation while circumventing the apoptotic effect of hypertonic treatment.

Discussion

Multipotent dedifferentiation of adipocytes holds strong promises to revolutionize regenerative medicine. However, the application potential is hampered by the unclear mechanisms and low efficiency [41]. Our work defined

(See figure on next page.)

Fig. 5 BML-284 induces dedifferentiation of adipocytes. **A** Representative images of adipocytes treated by BML-284 for the indicated time. Scale bar, 100 μ m. **B** Quantification of adipocytes losing all their clear lipid droplets during seven days of control or BML-284 culture. Error bars represent SD ($n = 3$, independent repeats). **C** and **D** Images (C) and quantification (D) of Oil Red O show adipocytes losing all their clear lipid droplets following indicated treatments for seven days. **E** Box plots depict the aspect ratio of indicated adipocytes ($n = 200$ cells) following control or BML-284 treatments. **F** RT-qPCR analysis of the expression of C/EBP β , PPAR γ , and adiponectin in control or BML-284 treated adipocytes. **G** RT-qPCR analysis of the expression of pluripotency markers Smad9, Esrrb and Sox2 in control or BML-284 treated adipocytes. **H** RT-qPCR analysis of the expression of Smad3, Col2a1 and Sox9 of isotonic and BML-284 treated adipocytes following chondrogenic induction. **I** Representative images of alkaline phosphatase (ALP) staining showing the osteogenic potential of the de-differentiated 3T3-L1 adipocytes following control or BML-284 treatments. **J** RT-qPCR analysis of the expression of ALP following osteogenic induction of control- or BML-284-treated 3T3-L1 adipocytes. **K** Representative results of annexin V/PI flow cytometry analysis of adipocytes receiving indicated treatments. **L** Bar graphs depict the proportions of cells in early-phase apoptosis in adipocytes receiving indicated treatments

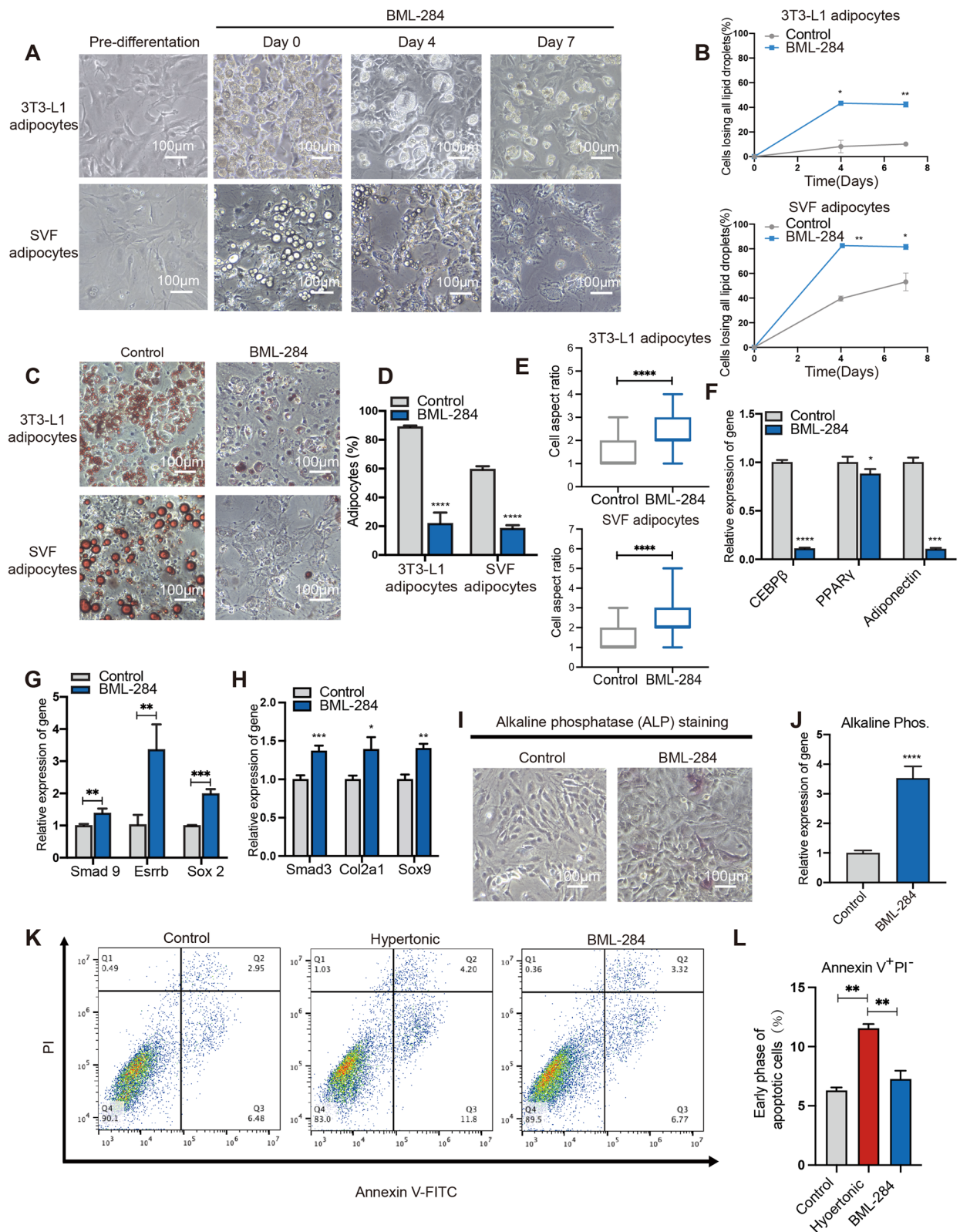


Fig. 5 (See legend on previous page.)

a novel signaling axis that promotes the multipotent dedifferentiation of adipocytes. High osmolarity induce the mitochondrial stress and prompts the adipocytes to release of mitochondria-containing EVs (Fig. 2), which in turn enhances the secretion of TNF- α as a pro-inflammatory cytokine during the stress response (Fig. 3). Importantly, we revealed that the Wnt/ β -catenin signaling was activated by TNF- α to drive the adipocyte dedifferentiation (Fig. 4). Furthermore, direct activation of Wnt/ β -catenin signaling by BML-284 could efficiently induce adipocyte dedifferentiation while circumventing the apoptotic effect of the hypertonic treatment (Fig. 5). Our results provide a mechanistic foundation for efficiently inducing adipocyte differentiation as a strategy in regenerative medicine.

Osmotic stress can take place in a diverse array of conditions with physiologic or pathologic influences on the adipocytes [42]. For example, hyperosmotic stress of adipocytes was reported to inhibit insulin signaling and induce insulin-resistance [43]. In addition, Zhu et al. reported that the adipocytes in breast cancer tissues could undergo the adipocyte mesenchymal transition (AMT) that generate multiple cell types constituting an inflammatory and tumor-promoting stroma [44]. Although the mechanism of AMT remains unclear, it is important to note that the osmotic stress and compression in breast cancer have been reported to activate β -catenin signaling and induce the adipocytes dedifferentiation with multi-lineage redifferentiation potentials [21]. Our results suggest that hypertonic MEVs mediate β -catenin activation and adipocytes dedifferentiation in response to osmotic stress (Fig. 4). It would be of interest to investigate whether hypertonic stress of mitochondria and MEVs of adipocytes are implicated in the malignant AMT of breast adipose tissue in vivo. This could provide a potential therapeutic target in the breast cancer microenvironment.

Recent studies have demonstrated that various cells could eject mitochondria to regulate homeostasis. For example, Nicolás-Ávila et al. found that cardiomyocytes release damaged mitochondria in extracellular vesicles (EVs) to maintain proper heart function [45]. We here report that hypertonic treatment of adipocytes could lead to EV-mediated mitochondrial ejection. Mechanistically, the fluctuation of the cellular osmolarity could perturb the ion homeostasis and electronic potential in mitochondria, leading to damages of the components. This is supported by the data that pyruvate could reduce the hypertonic MEVs (Fig. 2). Similarly, Rosina et al. have

reported that thermogenically stressed brown adipocytes eject dysfunctional mitochondrial parts in EVs to prevent failure of the thermogenic program [32]. It remains unclear about the cellular process and mechanisms of releasing mitochondrial components via EVs. It would be interesting to compare MEVs from different conditions for their components and activities in inducing adipocyte dedifferentiation. Accumulating evidence also indicate that adipocyte dedifferentiation plays an important role in tissue homeostasis. For example, Zhang et al. reported that dermal adipose tissue undergoes dedifferentiation and redifferentiation in hair cycle and wound healing [46]. In line with this, lineage tracing and single-cell RNA sequencing have revealed myofibroblasts derived from adipocytes during wound healing [47]. It is of interest to note that wound healing is accompanied by activation of the inflammatory cytokines including TNF- α and we found that the hypertonic MEVs promote the TNF- α \rightarrow β -catenin signaling axis in driving adipocytes dedifferentiation. In the studies of both Nicolás-Ávila et al. and Rosina et al., immune cells such as macrophages play a critical role in removing the ejected mitochondria and maintaining the homeostasis of the source tissue. Therefore, how MEVs function with the inflammation/immune system to induce adipocyte dedifferentiation in vivo would need further investigation. In addition, we showed that hypertonicity also induces apoptosis in adipocytes, which could be alleviated by direct activation of β -catenin. This suggests heterogeneity in the responses of adipocytes toward hypertonicity and ejected MEVs. Elucidating the mechanisms that dictate the apoptosis/dedifferentiation fate would pave the way for effectively harnessing adipocytes for regenerative medicine (Fig. 6).

Conclusion

Our study has shed new light on the mechanisms underlying the multipotent dedifferentiation of adipocytes, which holds great promise for regenerative medicine. We have identified a novel signaling axis involving high osmolarity-induced mitochondrial stress, EV-mediated mitochondrial ejection, TNF- α secretion, and Wnt/ β -catenin activation that promotes adipocyte dedifferentiation. We also demonstrated that direct activation of Wnt/ β -catenin signaling by BML-284 could efficiently induce adipocyte differentiation while circumventing

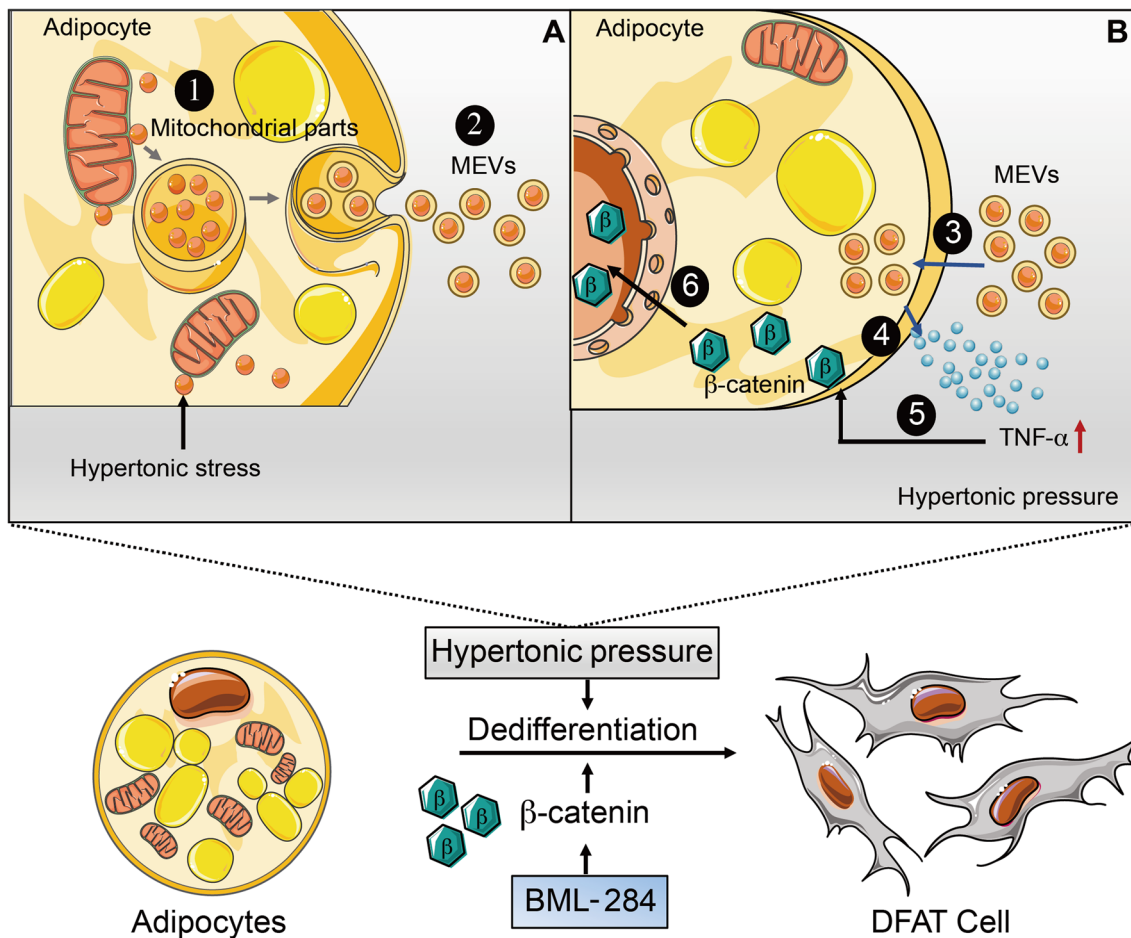


Fig. 6 Working model of adipocyte dedifferentiation induced by hypertonicity

the apoptotic effect of hypertonic treatment, providing a potential strategy for regenerative medicine applications.

Abbreviations

- SVF Stromal vascular fraction
- EVs Extracellular vesicles
- MEVs Mitochondrial extracellular vesicles
- DFAT Dedifferentiated fat cells
- ACK Ammonium–chloride–potassium
- PEG 300 Polyethylene glycol 300
- ALP Alkaline phosphatase
- C/EBPβ CCAAT/enhancer binding protein beta
- PPARγ Peroxisome proliferator-activated receptor gamma
- CD13 Aminopeptidase N
- Runx2 RUNX Family Transcription Factor 2
- Smad3 Mothers against decapentaplegic homolog 3
- Col2a1 Collagen Type II Alpha 1 Chain
- Sox9 SRY-Box Transcription Factor 9
- ATP Adenosine triphosphate
- NDUFA9 NADH:Ubiquinone Oxidoreductase Subunit A9
- UQCRC2 Ubiquinol-Cytochrome C Reductase Core Protein 2
- VDAC Voltage-dependent anion channel
- CD81 Cluster of Differentiation 81
- TNF-α Tumor Necrosis Factor-α
- IL-6 Interleukin 6
- RIP1 Receptor-interacting serine/threonine-protein 1

- CEBPA CCAAT/enhancer-binding protein alpha
- MCP-1 Monocyte chemoattractant protein-1
- Esrrb Estrogen Related Receptor Beta
- Sox2 Sex determining region Y-box 2
- Smad9 Mothers against decapentaplegic homolog 9

Supplementary Information

The online version contains supplementary material available at <https://doi.org/10.1186/s13287-023-03558-3>.

Additional file 1. Original western blot images.

Additional file 2. Supplementary Figures and Tables.

Acknowledgments

We thank the Laboratory Animal Research Unit of City University of Hong Kong for providing the technical supports.

Author contributions

G.L. and L.Z. designed the experiments. G.L., Y.W., Y.L.P., L.T., and M.H.C., performed experiments and data analysis. S.H. C., J. Z., J.Y.K. and L.W. provided materials and scientific inputs. All the authors wrote the article together. All authors read and approved the final manuscript.

Funding

This work was supported by grants from the Shenzhen Science and Technology Innovation Commission (JCYJ20210324133812034 to L.Z.) and the Shenzhen-Hong Kong Science and Technology Innovation Cooperation Zone Shenzhen Park Project (HZQB-KCZY2021017 to L.Z.), grants from The Tung Foundation Biomedical Sciences Centre (9609301 to L. Z. and 9609310 to J.Y.K.), and grants from the Research Grants Council of Hong Kong (21101917, 11103318, R1020-18 to L.Z. and 11101017 to J.Y.K.). The funding bodies played no role in the design of the study and collection, analysis, and interpretation of data and in writing the manuscript.

Availability of data and materials

The mass spectrometry proteomics data have been deposited to the ProteomeXchange Consortium via the iProX partner repository with the dataset identifier PXD04259. The data can be accessed through the permanent link: <https://www.iprox.cn/page/project.html?id=IPX0005941000>.

Declarations

Ethics approval and consent to participate

This study was approved by the Institutional Animal Research Ethics Subcommittee of City University of Hong Kong and Department of Health, The Government of The Hong Kong Special Administrative Region. (Approval number: AN-STA-00000135). The title of ethical approved project: "Investigating organ crosstalk in mouse obesity". Date of approval: 2023/1/11.

Consent for publication

Not applicable.

Competing interests

The authors declare no conflict of interests.

Author details

¹Department of Biomedical Sciences, College of Veterinary Medicine and Life Sciences, City University of Hong Kong, 83 Tat Chee Avenue, Kowloon, Hong Kong, China. ²Key Laboratory of Biochip Technology, Biotech and Health Centre, Shenzhen Research Institute of City University of Hong Kong, Shenzhen 518057, China. ³Medicinal Chemistry and Bioinformatics Center, Shanghai Jiao Tong University, School of Medicine, Shanghai 200025, China.

Received: 23 May 2023 Accepted: 2 November 2023

Published online: 20 December 2023

References

- Sakers A, De Siqueira MK, Seale P, Villanueva CJ. Adipose-tissue plasticity in health and disease. *Cell*. 2022;185:419–46.
- Bhaskaran K, Douglas I, Forbes H, dos-Santos-Silva I, Leon DA, Smeeth L. Body-mass index and risk of 22 specific cancers: a population-based cohort study of 5.24 million UK adults. *Lancet*. 2014;384:755–65.
- Gallagher EJ, LeRoith D. Obesity and diabetes: the increased risk of cancer and cancer-related mortality. *Physiol Rev*. 2015;95:727–48.
- Flock MR, Green MH, Kris-Etherton PM. Effects of adiposity on plasma lipid response to reductions in dietary saturated fatty acids and cholesterol. *Adv Nutr*. 2011;2:261–74.
- Sun K, Kusminski CM, Scherer PE. Adipose tissue remodeling and obesity. *J Clin Invest*. 2011;121:2094–101.
- Chen M, Lu P, Ma Q, Cao Y, Chen N, Li W, Zhao S, Chen B, Shi J, Sun Y, Shen H, Sun L, Shen J, Liao Q, Zhang Y, Hong J, Gu W, Liu R, Ning G, Wang W, Wang J. CTNBN1/beta-catenin dysfunction contributes to adiposity by regulating the cross-talk of mature adipocytes and preadipocytes. *Sci Adv*. 2020;6:eaax9605.
- Song T, Kuang S. Adipocyte dedifferentiation in health and diseases. *Clin Sci*. 2019;133:2107–19.
- Wang QA, Song A, Chen W, Schwalie PC, Zhang F, Vishvanath L, Jiang L, Ye R, Shao M, Tao C, Gupta RK, Deplancke B, Scherer PE. Reversible de-differentiation of mature white adipocytes into preadipocyte-like precursors during lactation. *Cell Metab*. 2018;28:282e283.
- Gustafson B, Smith U. Activation of canonical wingless-type MMTV integration site family (Wnt) signaling in mature adipocytes increases beta-catenin levels and leads to cell dedifferentiation and insulin resistance. *J Biol Chem*. 2010;285:14031–41.
- Bochet L, Lehuède C, Dauvillier S, Wang YY, Dirat B, Laurent V, Dray C, Guiet R, Maridonneau-Parini I, Le Gonidec S, Couderc B, Escourrou G, Valet P, Muller C. Adipocyte-derived fibroblasts promote tumor progression and contribute to the desmoplastic reaction in breast cancer. *Cancer Res*. 2013;73:5657–68.
- Bi P, Yue F, Karki A, Castro B, Wirbisky SE, Wang C, Durkes A, Elzey BD, Andrisani OM, Bidwell CA, Freeman JL, Konieczny SF, Kuang S. Notch activation drives adipocyte dedifferentiation and tumorigenic transformation in mice. *J Exp Med*. 2016;213:2019–37.
- Tang P, Virtue S, Goie JYG, Png CW, Guo J, Li Y, Jiao H, Chua YL, Campbell M, Moreno-Navarrete JM, Shabbir A, Fernandez-Real JM, Gasser S, Kemeny DM, Yang H, Vidal-Puig A, Zhang Y. Regulation of adipogenic differentiation and adipose tissue inflammation by interferon regulatory factor 3. *Cell Death Differ*. 2021;28:3022–35.
- Sun L, Goff LA, Trapnell C, Alexander R, Lo KA, Hacisuleyman E, Sauvageau M, Tazon-Vega B, Kelley DR, Hendrickson DG, Yuan B, Kellis M, Lodish HF, Rinn JL. Long noncoding RNAs regulate adipogenesis. *Proc Natl Acad Sci USA*. 2013;110:3387–92.
- Ross SE, Hemati N, Longo KA, Bennett CN, Lucas PC, Erickson RL, MacDougald OA. Inhibition of adipogenesis by Wnt signaling. *Science*. 2000;289:950–3.
- Christodoulides C, Lagathu C, Sethi JK, Vidal-Puig A. Adipogenesis and WNT signalling. *Trends Endocrinol Metab*. 2009;20:16–24.
- Choy L, Skillington J, Derynck R. Roles of autocrine TGF-beta receptor and Smad signaling in adipocyte differentiation. *J Cell Biol*. 2000;149:667–82.
- Cawthorn WP, Heyd F, Hegyi K, Sethi JK. Tumour necrosis factor-alpha inhibits adipogenesis via a beta-catenin/TCF4(TCF7L2)-dependent pathway. *Cell Death Differ*. 2007;14:1361–73.
- Sugihara H, Yonemitsu N, Miyabara S, Yun K. Primary cultures of unilocular fat cells: characteristics of growth in vitro and changes in differentiation properties. *Differentiation*. 1986;31:42–9.
- Cote JA, Lessard J, Pelletier M, Marceau S, Lesclleur O, Fradette J, Tchernof A. Role of the TGF-beta pathway in dedifferentiation of human mature adipocytes. *FEBS Open Biol*. 2017;7:1092–101.
- Guo M, Pegoraro AF, Mao A, Zhou EH, Arany PR, Han Y, Burnette DT, Jensen MH, Kasza KE, Moore JR, Mackintosh FC, Fredberg JJ, Mooney DJ, Lippincott-Schwartz J, Weitz DA. Cell volume change through water efflux impacts cell stiffness and stem cell fate. *Proc Natl Acad Sci USA*. 2017;114:E8618–27.
- Li Y, Mao AS, Seo BR, Zhao X, Gupta SK, Chen M, Han YL, Shih TY, Mooney DJ, Guo M. Compression-induced dedifferentiation of adipocytes promotes tumor progression. *Sci Adv*. 2020;6:5611.
- Li Y, Mao AS, Seo BR, Zhao X, Gupta SK, Chen M, Han YL, Shih TY, Mooney DJ, Guo M. Generation of the compression-induced dedifferentiated adipocytes (CiDAs) using hypertonic medium. *Bio Protoc*. 2021;11: e3920.
- Liang Z, He Y, Tang H, Li J, Cai J, Liao Y. Dedifferentiated fat cells: current applications and future directions in regenerative medicine. *Stem Cell Res Ther*. 2023;14:207.
- Mohammed D, Park CY, Fredberg JJ, Weitz DA. Tumorigenic mesenchymal clusters are less sensitive to moderate osmotic stresses due to low amounts of junctional E-cadherin. *Sci Rep*. 2021;11:16279.
- Shen JF, Sugawara A, Yamashita J, Ogura H, Sato S. Dedifferentiated fat cells: an alternative source of adult multipotent cells from the adipose tissues. *Int J Oral Sci*. 2011;3:117–24.
- van Dam H, Huguier S, Kooistra K, Baguet J, Vial E, van der Eb AJ, Herrlich P, Angel P, Castellazzi M. Autocrine growth and anchorage independence: two complementing Jun-controlled genetic programs of cellular transformation. *Genes Dev*. 1998;12:1227–39.
- Maacha S, Bhat AA, Jimenez L, Raza A, Haris M, Uddin S, Grivel JC. Extracellular vesicles-mediated intercellular communication: roles in the tumor microenvironment and anti-cancer drug resistance. *Mol Cancer*. 2019;18:55.
- Nunes P, Roth I, Meda P, Feraille E, Brown D, Hasler U. Ionic imbalance, in addition to molecular crowding, abates cytoskeletal dynamics and vesicle motility during hypertonic stress. *Proc Natl Acad Sci USA*. 2015;112:E3104-3113.

29. Xiao B, Deng X, Zhou W, Tan EK. Flow cytometry-based assessment of mitophagy using MitoTracker. *Front Cell Neurosci.* 2016;10:76.
30. McCommis KS, Finck BN. Mitochondrial pyruvate transport: a historical perspective and future research directions. *Biochem J.* 2015;466:443–54.
31. Abramov AY, Duchon MR. Mechanisms underlying the loss of mitochondrial membrane potential in glutamate excitotoxicity. *Biochim Biophys Acta.* 2008;1777:953–64.
32. Rosina M, Ceci V, Turchi R, Chuan L, Borcherding N, Sciarretta F, Sanchez-Diaz M, Tortolici F, Karlinsey K, Chiurchiu V, Fuoco C, Giwa R, Field RL, Audano M, Arena S, Palma A, Riccio F, Shamsi F, Renzone G, Verri M, Crescenzi A, Rizza S, Faienza F, Filomeni G, Kooijman S, Rufini S, de Vries AAF, Scaloni A, Mitro N, Tseng YH, Hidalgo A, Zhou B, Brestoff JR, Aquilano K, Lettieri-Barbato D. Ejection of damaged mitochondria and their removal by macrophages ensure efficient thermogenesis in brown adipose tissue. *Cell Metab.* 2022;34:533e512–548e512.
33. Maeda A, Fadeel B. Mitochondria released by cells undergoing TNF- α -induced necroptosis act as danger signals. *Cell Death Dis.* 2014;5:e1312.
34. Amari L, Germain M. Mitochondrial extracellular vesicles—origins and roles. *Front Mol Neurosci.* 2021;14:767219.
35. Todkar K, Chikhi L, Desjardins V, El-Mortada F, Pepin G, Germain M. Selective packaging of mitochondrial proteins into extracellular vesicles prevents the release of mitochondrial DAMPs. *Nat Commun.* 2021;12:1971.
36. Peruzzotti-Jametti L, Bernstock JD, Willis CM, Manferrari G, Rogall R, Fernandez-Vizarrá E, Williamson JC, Braga A, van den Bosch A, Leonardi T, Krzak G, Kittel A, Beninca C, Vicario N, Tan S, Bastos C, Bicci I, Iraci N, Smith JA, Peacock B, Muller KH, Lehner PJ, Buzas EI, Faria N, Zeviani M, Frezza C, Brisson A, Matheson NJ, Viscomi C, Pluchino S. Neural stem cells traffic functional mitochondria via extracellular vesicles. *PLoS Biol.* 2021;19:e3001166.
37. Brestoff JR, Wilen CB, Moley JR, Li Y, Zou W, Malvin NP, Rowen MN, Saunders BT, Ma H, Mack MR, Hykes BL Jr, Balce DR, Orvedahl A, Williams JW, Rohatgi N, Wang X, McAllaster MR, Handley SA, Kim BS, Doench JG, Zinselmeyer BH, Diamond MS, Virgin HW, Gelman AE, Teitelbaum SL. Intercellular mitochondria transfer to macrophages regulates white adipose tissue homeostasis and is impaired in obesity. *Cell Metab.* 2021;33:270e278–282e278.
38. Xu H, Sethi JK, Hotamisligil GS. Transmembrane tumor necrosis factor (TNF)- α inhibits adipocyte differentiation by selectively activating TNF receptor 1. *J Biol Chem.* 1999;274:26287–95.
39. Takada I, Kouzmenko AP, Kato S. Wnt and PPAR γ signaling in osteoblastogenesis and adipogenesis. *Nat Rev Rheumatol.* 2009;5:442–7.
40. Prins JB, Niesler CU, Winterford CM, Bright NA, Siddle K, O'Rahilly S, Walker NI, Cameron DP. Tumor necrosis factor- α induces apoptosis of human adipose cells. *Diabetes.* 1997;46:1939–44.
41. Jumabay M, Bostrom KI. Dedifferentiated fat cells: a cell source for regenerative medicine. *World J Stem Cells.* 2015;7:1202–14.
42. Yancey PH, Clark ME, Hand SC, Bowlus RD, Somero GN. Living with water stress: evolution of osmolyte systems. *Science.* 1982;217:1214–22.
43. Gual P, Gonzalez T, Gremeaux T, Barres R, Le Marchand-Brustel Y, Tanti JF. Hyperosmotic stress inhibits insulin receptor substrate-1 function by distinct mechanisms in 3T3-L1 adipocytes. *J Biol Chem.* 2003;278:26550–7.
44. Zhu Q, Zhu Y, Hepler C, Zhang Q, Park J, Gliniak C, Henry GH, Crewe C, Bu D, Zhang Z, Zhao S, Morley T, Li N, Kim DS, Strand D, Deng Y, Robino JJ, Varlamov O, Gordillo R, Kolonin MG, Kusminski CM, Gupta RK, Scherer PE. Adipocyte mesenchymal transition contributes to mammary tumor progression. *Cell Rep.* 2022;40:111362.
45. Nicolas-Avila JA, Lechuga-Vieco AV, Esteban-Martinez L, Sanchez-Diaz M, Diaz-Garcia E, Santiago DJ, Rubio-Ponce A, Li JL, Balachander A, Quintana JA, Martinez-de-Mena R, Castejon-Vega B, Pun-Garcia A, Traves PG, Bonzon-Kulichenko E, Garcia-Marques F, Cusso LAGN, Gonzalez-Guerra A, Roche-Molina M, Martin-Salamanca S, Crainiciuc G, Guzman G, Larrazabal J, Herrero-Galan E, Alegre-Cebollada J, Lemke G, Rothlin CV, Jimenez-Borreguero LJ, Reyes G, Castrillo A, Desco M, Munoz-Canoves P, Ibanez B, Torres M, Ng LG, Priori SG, Bueno H, Vazquez J, Cordero MD, Bernal JA, Enriquez JA, Hidalgo A (2020) A network of macrophages supports mitochondrial homeostasis in the heart. *Cell* 183:94–109e123
46. Zhang Z, Shao M, Hepler C, Zi Z, Zhao S, An YA, Zhu Y, Ghaben AL, Wang MY, Li N, Onodera T, Joffin N, Crewe C, Zhu Q, Vishvanath L, Kumar A, Xing C, Wang QA, Gautron L, Deng Y, Gordillo R, Kruglikov I, Kusminski CM, Gupta RK, Scherer PE. Dermal adipose tissue has high plasticity and undergoes reversible dedifferentiation in mice. *J Clin Invest.* 2019;129:5327–42.
47. Shook BA, Wasko RR, Mano O, Rutenberg-Schoenberg M, Rudolph MC, Zirak B, Rivera-Gonzalez GC, Lopez-Giraldez F, Zarini S, Rezza A, Clark DA, Rendl M, Rosenblum MD, Gerstein MB, Horsley V (2020) Dermal adipocyte lipolysis and myofibroblast conversion are required for efficient skin repair. *Cell Stem Cell* 26:880–895e886

Publisher's Note

Springer Nature remains neutral with regard to jurisdictional claims in published maps and institutional affiliations.

Ready to submit your research? Choose BMC and benefit from:

- fast, convenient online submission
- thorough peer review by experienced researchers in your field
- rapid publication on acceptance
- support for research data, including large and complex data types
- gold Open Access which fosters wider collaboration and increased citations
- maximum visibility for your research: over 100M website views per year

At BMC, research is always in progress.

Learn more biomedcentral.com/submissions

